A Model of a Quantum Particle in a Quantum Environment: A Numerical Study

Raffaele Carlone[1], Rodolfo Figari[2] and Claudia Negulescu[3],*

[1] *Università Federico II di Napoli, Dipartimento di Matematica e Applicazioni "R. Caccioppoli", MSA I-80126 Napoli, Italy.*

[2] *Università Federico II di Napoli, Dipartimento di Fisica e INFN Sezione di Napoli, MSA I-80126 Napoli, Italy.*

[3] *Université de Toulouse & CNRS, UPS, Institut de Mathématiques de Toulouse UMR 5219, F-31062 Toulouse, France.*

Abstract. We define and investigate, via numerical analysis, a one dimensional toy-model of a cloud chamber. An energetic quantum particle, whose initial state is a superposition of two identical wave packets with opposite average momentum, interacts during its evolution and exchanges (small amounts of) energy with an array of localized spins. Triggered by the interaction with the environment, the initial superposition state turns into an incoherent sum of two states describing the following situation: or the particle is going to the left and a large number of spins on the left side changed their states, or the same is happening on the right side. This evolution is reminiscent of what happens in a cloud chamber where a quantum particle, emitted as a spherical wave by a radioactive source, marks its passage inside a supersaturated vapour-chamber in the form of a sequence of small liquid bubbles arranging themselves around a possible classical trajectory of the particle.

1 Introduction

In this paper we investigate numerically the dynamics of a quantum particle interacting with a quantum environment. More precisely, we consider the semi-classical limit regime

---

Corresponding author. Email addresses: `raffaele.carlone@unina.it` (R. Carlone), `figari@na.infn.it` (R. Figari), `claudia.negulescu@math.univ-toulouse.fr` (C. Negulescu)

of the dynamics. With this we mean that the average initial kinetic energy of the particle is assumed to be very large with respect to the energy exchanged by the particle with the environment.

The paradigmatic physical system we have in mind is the Wilson cloud chamber, the prototype of a tracking chamber for elementary particle detection [6, 13–15]. Inside the chamber, a very energetic α-particle, emitted in a radially symmetric way by a radioactive source, ionizes atoms of a super-saturated vapor. In turn, the ionized atoms become condensation nuclei, triggering the formation of sequences of liquid drops. The tracks one observes in real experiments look quite explicitly as classical particle trajectories.

In the early days of quantum mechanics Darwin, Heisenberg and Mott were the first to point out the seemingly paradoxical circumstance of an initial radially symmetric quantum state evolving into wave packets concentrated around classical trajectories. In different ways, they suggested that the problem could be faced taking into consideration that the wave function does not evolve in real space, but rather in the configuration space of the entire quantum system. This somehow obvious but extremely far-reaching intuition, exploited by Mott in his seminal work [21], remained unnoticed for decades.

More recently, researchers analyzed the cloud chamber problem focusing on different aspects of the interaction of a microscopic quantum system with a macroscopic one.

- **Decoherence:** the initial state of the α-particle can be seen as a superposition of coherent states each one having a well localized momentum direction. The superposition is initially strongly coherent: in absence of any interaction with the environment, two coherent states might interfere in a double-slit experiment. On the other hand, coherent states heading in different directions generate macroscopic ionization in different regions of the environment. Due to this particle-environment interaction, the state of the whole system evolves into an incoherent superposition of states supported in distant regions of the environment configuration space, in such a way that interference effects become negligible. For a general presentation of the decoherence phenomenon see e.g. [17] and references therein. For details on collisional decoherence in a tracking chamber we refer to the book [12].

- **Non demolition measure:** a microscopic system (e.g. a quantum particle) is said to undergo a non demolition measure if there is a basis of its states which are left unchanged by the interaction with the probe (the measurement apparatus). At the same time, in order to work as a measurement apparatus, the probe should evolve in different final states for different particle states in the basis. Some authors analyzed recently the effect of repeated non demolition measures and its relation with the "collapse" of the wave function in a quantum measurement [2]. In this language, the process described above can be rephrased in the following way: each coherent state with a well defined momentum direction is an element of the basis. For a very high average initial energy (semi-classical conditions) each state of the basis evolves almost freely in each weakly-inelastic scattering process, whereas the environment reacts in different ways according to the average momentum direction

of each coherent state. Repeated scattering processes will bring to the collapse of the wave function on one of the states in the superposition.

Besides the fundamental aspects mentioned before, other motivations for understanding the dynamics of decoherence come from several technological applications exploiting quantum coherence, such as quantum computers, electron spin resonance, nuclear magnetic resources and so on. Efforts are hence made in order to try to curb the destructive role of decoherence in such applications.

To model and give rigorous mathematical results concerning the dynamics of a quantum particle in a many body quantum environment is a difficult task [25]. In the second half of the last century, few attempts to define simplified solvable particle-environment models were made, starting from the seminal papers [16, 18, 19]. More recent investigations on the same line are [1, 4, 8, 9, 11, 12, 22, 26]. In all these models the environment is made of either two or more level "atom"-arrays (spins or oscillators) or of a gas of light particles.

In the following, we present a simple one dimensional model of a cloud chamber. The environment consists of an array of two level quantum systems (sometimes referred to as atoms or spins) kept in fixed positions. The particle initial state is made of two identical wave packets concentrated in the origin (where a radioactive source is located) and moving away from the origin with opposite average momentum. All the atoms are initially in their ground state. The interaction particle-environment is modelled by multi-channel point potentials [5], allowing energy exchanges between the particle and the atoms.

This is one of the simplest particle-environment model, permitting a reasonable numerical study of the decoherence phenomenon. Numerical simulations of the whole system evolution will be presented and confirm that after the interaction process has taken place, the solution, apart for negligible terms, has the form of an incoherent sum of three states describing alternative histories of the environment: either no significative atom excitation has taken place or only atoms on one side of the origin are found in an excited state. Furthermore, the numerical results show that the higher the number of environment constituents is (spins or atoms), the more effective is the environment induced decoherence. This is a new and important achievement of the present work. A different model has been investigated in [1] to study the decoherence effects induced by successive two-body heavy-light particle interactions. The model presented here is somehow more realistic, as it examines the real dynamics of the whole system, where simultaneous particle-environment interactions are allowed.

The paper is organized as follows. Section 2 contains a concise introduction of the particle-environment model presented in [5]. In Section 3 we give details on the space-time discretization of the above model, used in the numerical computation of the wave-function solutions. The results of the numerical simulations are presented in Section 4. Comments on these results and achievable future extensions of this work are presented in the final section.

2   Multi-channel point interactions

In the present section we introduce a simple mathematical model of a one dimensional quantum gas inside a Wilson-chamber. We analyze the dynamics of the wave-function $\Psi(t,x)$ representing the whole quantum-mechanical system, made of an α-particle and its environment, which has the role of detecting the particle passage. The interaction particle-environment is modeled via multi-channel point interactions.

2.1   The model

We consider a quantum particle moving on a line and interacting with an array of N localized spins. In mathematical terms, the time evolution of this toy model is given by the Schrödinger equation

$$\begin{cases} \mathbf{i}\hbar\partial_t\Psi = H\Psi, \\ \Psi(0,\cdot) = \Psi_0, \end{cases} \tag{2.1}$$

where Ψ is the wave-function describing the whole quantum system, $\hbar$ is the Planck constant and $H: D(H) \subset \mathcal{H} \to \mathcal{H}$ is the Hamiltonian whose domain and action will be defined later on.

The space of the system state is the Hilbert-space $\mathcal{H} = L^2(\mathbf{R}) \otimes \mathbb{S}_N$. Here,

$$\mathbb{S}_N = \underbrace{\mathbb{C}^2 \otimes \cdots \otimes \mathbb{C}^2}_{N \text{ times}}$$

is the configuration space of the environmental spins, whereas $L^2(\mathbf{R})$ is the configuration space of the α-particle. The N spins are assumed to be localized in the positions $Y = \{y_1, \cdots, y_N\}$ with $y_j \in \mathbf{R}$ for all $j \in \mathcal{J} := \{1, \cdots, N\}$.

Let us denote by

$$\hat{\sigma}^{(3)} = \begin{pmatrix} 1 & 0 \\ 0 & -1 \end{pmatrix}$$

the third Pauli matrix. The j-th spin state space $\mathbb{C}^2$ can be viewed as the complex linear span of the spin eigenstates χ_{σ_j} corresponding to the eigenvalues $\sigma_j = \pm 1$ of $\hat{\sigma}^{(3)}$, and representing the "spin up" and "spin down" states.

The state space $\mathbb{S}_N$ of the entire spin array will be the complex linear span of the basis vectors $\chi_{\underline{\sigma}} = \chi_{\sigma_1} \otimes \cdots \otimes \chi_{\sigma_N}$, where $\underline{\sigma} := (\sigma_1, \cdots, \sigma_N) \in \mathcal{S} := \{\pm 1\}^N$ denotes one of the $M := 2^N$ possible spin configurations.

With this notation, the system consisting of the quantum particle and the N spins is described by the wave-function

$$\Psi = \sum_{\underline{\sigma} \in \mathcal{S}} \psi_{\underline{\sigma}} \otimes \chi_{\underline{\sigma}}, \qquad \Psi \in \mathcal{H}, \tag{2.2}$$

where the sum runs over all possible spin configurations of $\underline{\sigma} \equiv (\sigma_1, \cdots, \sigma_N)$. In this decomposition each $\psi_{\underline{\sigma}} \in L^2(\mathbf{R})$ represents the wave function of the particle when the spin configuration is $\underline{\sigma}$.

Alternatively, in the following we will use for the state of our quantum system the vectorial notation

$$\Psi = (\psi_{\underline{\sigma}_1}, \cdots, \psi_{\underline{\sigma}_M})^t = (\psi_{\underline{\sigma}})_{\underline{\sigma} \in \mathcal{S}} \in (L^2(\mathbf{R}))^M.$$

Correspondingly the Hamiltonian in (2.1) will then take the form of a $M \times M$ matrix.

The dynamics of the system is governed by the total Hamiltonian

$$H = H_0 + H_I, \tag{2.3}$$

which is decomposed into two distinct parts, H_0 describing the free independent evolution of the particle and of the spins, and H_I describing the particle-environment interaction. Furthermore, the interaction Hamiltonian H_I will be decomposed into two parts: a zero range interaction H_D, supported by the set of the spin positions, and a particle-spin interaction H_F.

A rigorous characterization of the spin-dependent point interaction Hamiltonian we are going to use in the following, is given in [5, Theorem 1]. Here we shall limit ourselves to recall the statement of the theorem in the one-dimensional case.

Let $\underline{\alpha} := (\alpha_1, \cdots, \alpha_N)$ with $\alpha_j \in \mathbf{R}^+ \, \forall j \in \mathcal{J}$ be any multi-index of non-negative real numbers; let β, ρ be two non-negative real numbers, and let us define $\underline{\alpha} \cdot \underline{\sigma} := \sum_{j=1}^{N} \alpha_j \sigma_j$.

The operator $H : D(H) \subset \mathcal{H} \to \mathcal{H}$ with domain

$$D(H) = \left\{ \Psi = \sum_{\underline{\sigma} \in \mathcal{S}} \psi_{\underline{\sigma}} \otimes \chi_{\underline{\sigma}} \in \mathcal{H} \,|\, \psi_{\underline{\sigma}} \in H^2(\mathbb{R} \backslash Y) \quad \forall \underline{\sigma} \in \mathcal{S}; \right. \tag{2.4}$$

$$\psi_{\underline{\sigma}}(y_j^+) = \psi_{\underline{\sigma}}(y_j^-) = \psi_{\underline{\sigma}}(y_j), \quad \forall \underline{\sigma} \in \mathcal{S}, \, \forall j \in \mathcal{J}, \tag{2.5}$$

$$\psi_{\underline{\sigma}}'(y_j^+) - \psi_{\underline{\sigma}}'(y_j^-) = \beta \psi_{\underline{\sigma}}(y_j) - 2\mathbf{i} \sigma_j \rho \psi_{\underline{\sigma}'}(y_j), \quad \forall \underline{\sigma}, \underline{\sigma}' \in \mathcal{S}, \tag{2.6}$$

$$\left. \text{such that } \sigma_j \neq \sigma_j', \sigma_k = \sigma_k' \, \forall k \neq j \right\}, \tag{2.7}$$

and action

$$H\Psi := \sum_{\underline{\sigma} \in \mathcal{S}} \left(-\frac{\hbar^2}{2m} \triangle + \underline{\alpha} \cdot \underline{\sigma} \right) \psi_{\underline{\sigma}} \otimes \chi_{\underline{\sigma}}, \qquad x \in \mathbb{R} \backslash Y, \tag{2.8}$$

is a selfadjoint operator.

In (2.4) we made use of the standard notation to specify the limit from the left or from the right, *i.e.* $\lim_{y \to y_j^{\pm}} \psi_{\underline{\sigma}}(y) =: \psi_{\underline{\sigma}}(y_j^{\pm})$.

Few relevant properties of the dynamics generated by the Hamiltonian (2.4)-(2.8) are worthy of remark:

- The evolution of the particle wave packet is free outside the points where the spins are located;

- The quantity $2\alpha_j$ represents the difference in energy between two spin configurations differing only in the value of the j-th spin. For simplicity reasons we will use in the following $\alpha_j = \alpha \ \forall j \in \mathcal{J}$ with $\alpha \in \mathbf{R}^+$;

- The parameter β represents the strength of the point interaction in any point $y_j \in Y$;

- The parameter ρ is a measure of the effectiveness of the interaction in rotating the spin at the particle passage;

- The interaction Hamiltonian has non vanishing matrix elements only between states whose spin configurations are equal or differ in one point only. This implies, at first order in perturbation theory, that only transitions of this kind have non zero probability.

Finally, let us specify the initial condition of the Cauchy problem (2.1). We assume that the α-particle and the environment are initially decoupled, *i.e.*

$$\Psi(0) = (\psi_{\underline{\sigma}_1}, 0, \cdots, 0)^t, \quad \underline{\sigma}_1 = \{-\}^N, \tag{2.9}$$

with the quantum particle initial wave packet given by

$$\psi_{\underline{\sigma}_1}(0,x) := c[f(x)e^{-\mathbf{i}\frac{p_0}{\hbar}x} + f(x)e^{\mathbf{i}\frac{p_0}{\hbar}x}], \tag{2.10}$$

where $c > 0$ is a normalization constant, p_0 is the particle average momentum and

$$f(x) := \begin{cases} e^{-\frac{|x|^2}{4\sigma^2}}, & x \in (-a,a), \ a,\sigma \in (0,\infty), \\ 0, & \text{elsewhere.} \end{cases}$$

The initial condition (2.9)-(2.10) expresses the fact that at time zero all spins are in the "down" state while the particle state is the superposition of two identical gaussian wavepackets moving in opposite directions with average momentum $\pm p_0$. Because of the presence of the Hamiltonian H_I this initial fully decoupled condition state will evolve into an entangled state which cannot be any longer written in product form.

Note that the initial condition belongs to the operator domain $D(H)$ (more precisely, it differs slightly from functions in the domain, due to the truncation of the gaussian). As a consequence, the state of the quantum system evolves remaining constantly in $D(H)$. In particular, the boundary conditions in (2.4) are satisfied at any time.

3 Numerical discretization

Let us now present in this section the numerical scheme we used in order to simulate the evolution of the system described in Section 2, in other words to resolve the Schrödinger equation (2.1) associated with (2.4)-(2.10). The results obtained with this scheme will be presented and analyzed in Section 4.

At this point, we would like to emphasize the difficulties in simulating the decoherence phenomenon. The first challenge comes from the limited numerical resources (memory) available in order to take into account for a multi-body quantum environment, in particular more than $N = 14$ spin-detectors becomes prohibitively expensive, with the scheme we shall present. To deal with the physically interesting case $N \to \infty$, one has to think of a different manner of modeling the Wilson-chamber, or to work out an analytical model to investigate the asymptotic dynamics of the system as $N \to \infty$. We plan to come back to this subject in future work. Here we limit ourselves to present preliminary results for $N \le 14$.

Moreover, the study of the decoherence process relies strongly on the specific system-environment interaction mechanism. In fact, the physical parameters of our model have to be chosen with care, in order to be able to estimate numerically the dynamical evolution of decoherence. In the same sense, even the discretization parameters $(\Delta t, \Delta x)$ have to be chosen carefully: on one hand, large enough to have tractable numerical simulations, and on the other hand small enough to be sure to get correct physical results. The choice of all these parameters will be discussed in Section 4.

3.1   Space-time discretization

For numerical simulations, we had to truncate the space domain from **R** to $\Omega := (-L, L)$, $L > 0$, and impose boundary conditions in $x = \pm L$. For simplicity reasons homogeneous Neumann boundary conditions are chosen in the following and the simulation domain as well as the simulation time are set such that the α-particle is not reaching the border, in order to avoid reflection effects coming from the boundaries. In this manner, one can think of the α-particle as evolving on the whole **R**-line.

Let us now discretize the simulation domain $[0, T] \times \Omega$ in the following homogeneous manner

$$-L =: x_1 \le \cdots \le x_i \le \cdots x_{N_x} := L, \quad x_i := -L + (i-1)\Delta x, \quad \Delta x := \frac{2L}{N_x - 1},$$

$$0 =: t_0 \le \cdots \le t_k \le \cdots t_K := T, \quad t_k := k\Delta t, \quad \Delta t := T/K.$$

Starting from the known initial condition $\Psi(0, \cdot) : [-L, L] \to \mathbb{C}^M$, where $M := 2^N$ is the number of possible spin configurations, we are searching at each time step t_k, $k = 1, \cdots, K$, for an approximation of the vectorial unknown $\Psi(t_k, x_i) \in \mathbb{C}^M$ in each point $x_i \in [-L, L]$, $i = 1, \cdots, N_x$, meaning $N_x * M$ scalar unknowns. This approximation shall be denoted simply by $\Psi_i^k \in \mathbb{C}^M$.

For the points far away from the detectors one can discretize the Schrödinger equation, associated with the Hamiltonian given by (2.8), via the second-order, unconditionally stable Crank-Nicolson scheme

$$\mathbf{i}\hbar \frac{\Psi_i^{k+1} - \Psi_i^k}{\Delta t} = -\frac{\hbar^2}{4m} \left(\frac{\Psi_{i+1}^{k+1} - 2\Psi_i^{k+1} + \Psi_{i-1}^{k+1}}{(\Delta x)^2} + \frac{\Psi_{i+1}^k - 2\Psi_i^k + \Psi_{i-1}^k}{(\Delta x)^2} \right) + \mathbb{D}_\alpha \frac{\Psi_i^{k+1} + \Psi_i^k}{2}, \quad (3.1)$$

where $i = 1, \cdots, N_x$ such that $x_i \notin Y$. Here $\mathbb{D}_\alpha \in \mathbf{R}^{M \times M}$ is a diagonal matrix whose entries correspond to the different energy levels of the spin-channels and are given by

$$\mathbb{D}_{\alpha,\underline{\sigma}} := \alpha \sum_{j=1}^{N} \sigma_j, \quad \forall \underline{\sigma} \in \mathcal{S}.$$

Remark moreover that the homogeneous Neumann boundary conditions impose for the ghost points $\Psi_0^k = \Psi_2^k$ as well as $\Psi_{N_x+1}^k = \Psi_{N_x-1}^k$ for all $k \in \{1, \cdots, K\}$. This discretization yields $N_x - N$ vector-equations for the wave-function $\Psi(t_k, x_i) \in \mathbb{C}^M$ with $x_i \notin Y$. Missing are now N vector equations.

In the points where the detectors are located, i.e. $x_i = y_j$, one has to take into account for the effects of the point interaction as well as of the possibility of a crossing to the different channels corresponding to the flipped spin (see (2.4)). In the following, we shall denote by $i_j \in \{1, \cdots, N_x\}$ the index of the detector $y_j \in Y$, i.e. $y_j = x_{i_j}$ for all $j \in \mathcal{J}$. To discretize the particle-environment dynamics in a detector-point $y_j \in Y$, let us integrate the free Schrödinger equation in the two intervals around this point $(y_j - \Delta x/2, y_j)$ and $(y_j, y_j + \Delta x/2)$ and sum up the results. This leads to

$$\mathbf{i}\hbar \partial_t \int_{y_j - \Delta x/2}^{y_j} \Psi dx \approx (\Delta x/2) \mathbf{i}\hbar \partial_t \Psi(y_j)$$

$$\approx -\frac{\hbar^2}{2m} \left[\partial_x \Psi(y_j^-) - \partial_x \Psi(y_j - \Delta x/2) \right] + \frac{\Delta x}{2} \mathbb{D}_\alpha \Psi(y_j),$$

$$\mathbf{i}\hbar \partial_t \int_{y_j}^{y_j + \Delta x/2} \Psi dx \approx (\Delta x/2) \mathbf{i}\hbar \partial_t \Psi(y_j)$$

$$\approx -\frac{\hbar^2}{2m} \left[\partial_x \Psi(y_j + \Delta x/2) - \partial_x \Psi(y_j^+) \right] + \frac{\Delta x}{2} \mathbb{D}_\alpha \Psi(y_j).$$

Summing up these formulae, yields for all $j \in \mathcal{J}$

$$(\Delta x) \mathbf{i}\hbar \partial_t \Psi_{i_j} = -\frac{\hbar^2}{2m} \left[\partial_x \Psi(y_j + \Delta x/2) - \partial_x \Psi(y_j - \Delta x/2) - \partial_x \Psi(y_j^+) \right.$$

$$\left. + \partial_x \Psi(y_j^-) \right] + (\Delta x) \mathbb{D}_\alpha \Psi_{i_j}.$$

Using now the boundary conditions on the detector positions, we get for each $j \in \mathcal{J}$ and each spin-configuration pair $\underline{\sigma}, \underline{\sigma}' \in \mathcal{S}$ verifying $\sigma_j \neq \sigma_j'$, and $\sigma_k = \sigma_k'$ for all $k \neq j$,

$$\mathbf{i}\hbar \partial_t \psi_{\underline{\sigma}, i_j} = -\frac{\hbar^2}{2m} \left[\frac{\psi_{\underline{\sigma}, i_j+1} - \psi_{\underline{\sigma}, i_j}}{(\Delta x)^2} - \frac{\psi_{\underline{\sigma}, i_j} - \psi_{\underline{\sigma}, i_j-1}}{(\Delta x)^2} - \frac{\beta}{\Delta x} \psi_{\underline{\sigma}, i_j} + 2\mathbf{i} \frac{\sigma_j \rho}{\Delta x} \psi_{\underline{\sigma}', i_j} \right] + \mathbb{D}_{\alpha, \underline{\sigma}} \psi_{\underline{\sigma}, i_j}, \quad (3.2)$$

yielding after the semi-discretization in time (Crank-Nicolson) the missing N vector-equations. Let us remark here that the discretization (3.2) is very similar to (3.1), in particular for $\beta = 0$ and $\rho = 0$ one gets exactly the free evolution discretization (3.1), which

is somehow consistent. The terms related to β, ρ and α express the fact that there is an energy exchange between the different spin-channels. Note furthermore that the Crank-Nicolson scheme has the essential property of preserving the discrete $||\cdot||_2$ norm, which is a considerable advantage in the present case.

The discretization (3.1)-(3.2) gives rise to a sparse matrix, consisting of M tridiagonal blocks, corresponding to the discretization of the Hamiltonian part $H_0 + H_D$, and N values per bloc localized outside the blocs and distributed in a well-defined manner, corresponding to the discretization of the particle-detectors interaction part H_F. The resolution of this sparse linear system $((3N_x - 2)M + NM$ non-zero elements) has been performed by means of the direct MUMPS solver (LU-decomposition). In the case one wants to increase the number of environmental spins above $N = 14$, more performant solvers have to be used, as for example the iterative Krylov solver, based on preconditioning techniques. However, doing in this manner shall only permit to slightly increase the number of spin-detectors N, and will only enable to confirm the tendency of our results. A better way to do, will be to study the asymptotic behaviour of our model, as $N \to \infty$, which will be done in future works.

4   Numerical results

Aim of the present section is to use the previously introduced numerical scheme in order to study the creation of "tracks" in our simplified Wilson-chamber model. As mentioned earlier, the meaning of a pattern formation in the present model is the following: a track is defined as the ionization (spin flip) of more than one atom/spin on only one side of the initial α-particle position $x_0 = 0$.

The parameters used for these simulations are summarized in Table 1. The choice of the parameters is related to some physical constraints, corresponding to the specific situation we want to describe. In particular, the spin-detectors are divided into two groups, located around $\pm D$, in a symmetric way with respect to the origin of the spherical wave ($x_0 = 0$). The distance between nearest spins in one group is called d. Furthermore, we suppose that the parameters satisfy the following assumptions:

$$\beta \ll 1/d, \qquad d < \sigma \ll D.$$

A small β denotes a very weak energy exchange between particle and environment guaranteeing the non demolition character of the interaction (in fact in dimension 1 it could be put equal to zero). The wave packet initial variance σ is chosen of the same order of magnitude of each spin cluster size. This means that we are in a situation where the particle is interacting simultaneously with the majority of the spins in each cluster. Moreover, the last inequality implies that the support of the wave packet has negligible intersection with the scatterer arrays until a finite flight-time, in which it reaches the spin clusters, is elapsed. Till then, the flipping probability is going to be negligible.

Finally, let us remark that the distances and simulation time have been chosen in such a way that before the final time t_* the α-particle, with high probability, has moved

Table 1: Parameters used in the numerical simulations.

L	$3/2$	$N_x, \Delta x$	$1000, 3*10^{-3}$
$t_\star$	0.065	$N_t, \Delta t$	$350, 1.8*10^{-4}$
ε	10^{-1}	$\hbar, m$	$\varepsilon, 1$
N	$4,6,8,10,12,14$	y_j	$\pm D \pm (2k+1)d/2, k=0,1,2,\cdots$
D	$L/3$	d	ε/N
x_0	0	p_0	$4/3\varepsilon$
σ	$\varepsilon/4$	β	ε^4
ρ	$r\varepsilon^{-2}, r \in [0.25, 0.75]$	α	ε^4

Table 2: Sum of probabilities $||\psi_{\underline{\sigma}}(t_\star)||^2_{L^2(\Omega)}$ according to specific configurations $\underline{\sigma} \in \mathcal{S}$, the sum over all configurations $\underline{\sigma} \in \mathcal{S}$ being equal to one.

$\rho = \varepsilon^{-2}/2, N$	Left/Right Cumulative	One spin	Unchanged	$2*LRC+OS+UC$
4	0.0325685025765	0.275253381822	0.659609415084	0.9999998020590
6	0.0732817073769	0.459327397789	0.394108332939	0.9999991454818
8	0.136249083320	0.467653883264	0.259847521850	0.9999995717540
10	0.178222289956	0.431768410329	0.211787009757	0.9999999999980
12	0.211022969661	0.429493203402	0.148460857272	0.9999999999960
14	0.226597325639	0.417498227100	0.129307121622	1.0000000000000

over all spin-detectors, but has not reached the border of the domain, so that disturbing secondary effects (like reflections) related to the boundaries are avoided.

Starting our simulations with the initial condition given in (2.10), which corresponds to a situation with all spin-detectors in a "down"-position, we are firstly interested in the probabilities of some specific spin configurations, at the final time $t_\star = 0.065$. The aim is to observe if the configurations corresponding to the creation of a track have a larger probability than other possible configurations. Some of these probabilities obtained with our numerical simulations are summarized in Table 2 (for $\rho = 50$) and Fig. 1 (for $\rho = 60$).

The quantities listed in Table 2 correspond to the following definitions:

- **N** is the number of spin-detectors distributed symmetrically with respect to the wave-packet initial position ($x_0 = 0$).

- **Left/Right Cumulative (LRC)** corresponds to the total probability of all configurations with flipped spins only on one side of x_0 (either on the left or on the right), excluding the case of a single spin flip, at final time $t_\star$.

- **One spin (OS)** corresponds to the total probability, at final time t_*, of all the configurations, in which only one spin has flipped.

- **Unchanged (UC)** is the probability of the configuration in which nothing happened during the simulation time, i.e. all the spins remained in the low energy state.
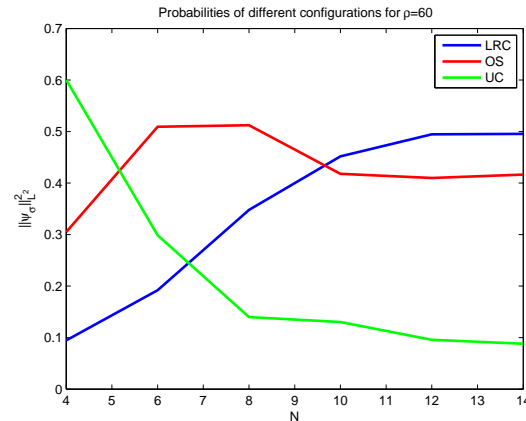
Figure 1: Plot of the $2*LRC$, OS and UC probabilities at final time $t_\star$, as a function of N and for $\rho = 60$.

- **Multiple tracks (MT)** is the total probability of the configurations in which spins on both side have moved to a configuration of higher energy $MT = 1 - 2*LRC - OS - UC$.

We considered independently the case where only one spin flipped with respect of the initial condition (OS). In fact, for a small total number of spins, the probability that only one spin have flipped is quite large. Nevertheless, it would be misleading to consider this case as a sign of a track on a specific side, taken into account that "one" point is always on a single side with respect of the origin. Notice however that with respect to the total number of spins we are able to manage, "one" is not a small percentage of points on one side of the origin.

What can be observed from the values in Table 2 and Fig. 1 is that the probability of observing a track on the right or on the left ($2*LRC$) is a strictly increasing function with the number of spins N, and that for each N this value is much larger than the probability to have no track formation (MT). Let us also remark that the sensitivity of the "device" is increasing with the number of the detectors, as it is clear from the fact that the probability of having no spin flip (UC) is strictly decreasing for increasing N. It is also worth notice that the "One-Spin" configuration is a non-monotone function with respect to N. In particular, there is a threshold value for N above which the probability OS starts to decrease. In fact, the number of configurations with more than one spin in the upper energy state on each side of the origin increases much faster than N. As a consequence, the probability that an almost unchanged wave packet (semi-classical conditions) causes multiple "ionization" increases, whereas the probability of a single ionization is expected to go to zero for large N.

In order to understand better the influence of the most significant parameters for the decoherence rate enhancement, we carried out other simulations, firstly varying the ρ-values for fixed number of spin-detectors N. These results are presented in Table 3

Table 3:   Sum of probabilities $||\psi_{\underline{\sigma}}(t_\star)||^2_{L^2(\Omega)}$ according to specific configurations $\underline{\sigma} \in \mathcal{S}$, for several ρ and N values. The sum of all configurations (for fixed ρ and N) is equal to one.

$N\!=\!6,\rho$	Left/Right Cumulative	One spin	Unchanged	$2*LRC\!+\!OS\!+\!UC$
75	0.109622994819	0.541164020727	0.239589989614	0.999999999979
50	0.0732817073769	0.459327397789	0.394108332939	0.9999991454818
25	0.0103574748581	0.193411720705	0.785873329578	0.9999999999992
$N\!=\!8,\rho$	Left/Right Cumulative	One spin	Unchanged	$2*LRC\!+\!OS\!+\!UC$
75	0.197957193495	0.534889312125	0.0691963008808	0.9999999999958
50	0.13624939796	0.467653682229	0.25984752185	0.999999999999
25	0.0200483456577	0.234013722944	0.725889585739	0.9999999999984
$N\!=\!10,\rho$	Left/Right Cumulative	One spin	Unchanged	$2*LRC\!+\!OS\!+\!UC$
75	0.256357991502	0.396021737286	0.0912622797074	0.9999999999974
50	0.178222289956	0.431768410329	0.211787009757	0.999999999998
25	0.0315466612839	0.268722187965	0.668184489466	0.9999999999988
$N\!=\!12,\rho$	Left/Right Cumulative	One spin	Unchanged	$2*LRC\!+\!OS\!+\!UC$
75	0.260042860561	0.391267684323	0.0886465945538	0.9999999999988
60	0.247268176496	0.409755032396	0.095708614611	0.999999999999
50	0.210785027601	0.429140888943	0.149289055854	0.999999999999
$N\!=\!14,\rho$	Left/Right Cumulative	One spin	Unchanged	$2*LRC\!+\!OS\!+\!UC$
60	0.247778838994	0.416465157958	0.0879771640541	1.00000000000
50	0.226597325639	0.4174982271	0.129307121622	1.00000000000
40	0.171978609852	0.412352635451	0.243690144846	1.00000000000

as well as in Figs. 2-3. We observe that with increasing ρ the *LRC*-probability becomes larger, whereas the *UC*-probability becomes smaller. This is rather consistent with the fact, that larger ρ means a larger rotation in each spin state space so that the pattern formation becomes more visible. The evolution of the *OS*-probability shows that the threshold value of N, above which this probability starts to decrease, changes with ρ. For larger ρ-values this threshold value diminishes.

In a final study, we were interested in the time-evolution of some wave-function components $\psi_{\underline{\sigma}}$ corresponding to a specific spin-configuration $\underline{\sigma} \in \mathcal{S}$. In particular one is interested in the comparison of the probabilities with which the initial state $\psi_{\underline{\sigma}_1}$ with all spins in the low energy state "down" ($\underline{\sigma}_1 := \{-\}^N$), transforms into some specific configurations, as for example the Left/Right Cumulative configurations or the One-Spin configurations. We represented in Figs. 4-5 the time evolution of these probabilities $\int_{-L}^{L} |\psi_{\underline{\sigma}}(t,x)|^2 dx$, for resp. $N\!=\!6,8,10,12,14$ spin-detectors and $\rho\!=\!60$. As expected, the probabilities start to increase at the moment, where the α-particle reached the spin-detectors, i.e. at approximately $t\!=\!D/p_0\!=\!0.0375$.
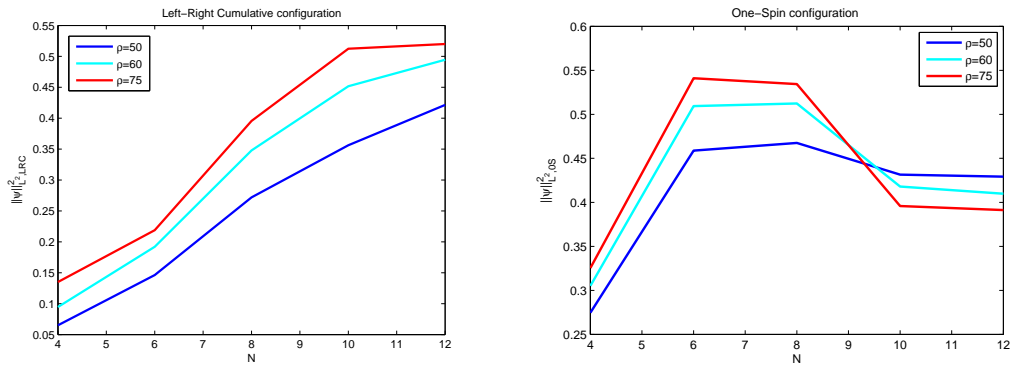
Figure 2: Plot of the $2*LRC$ and OS probabilities at final time $t_\star$, as a function of N and for $\rho = 50,60,75$.
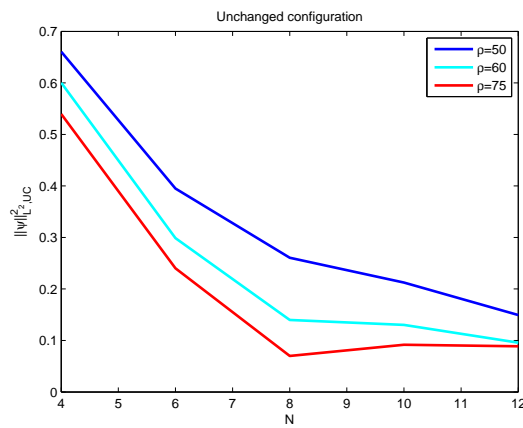

Figure 3: Plot of the UC probability at final time $t_\star$, as a function of N and for $\rho = 50,60,75$.
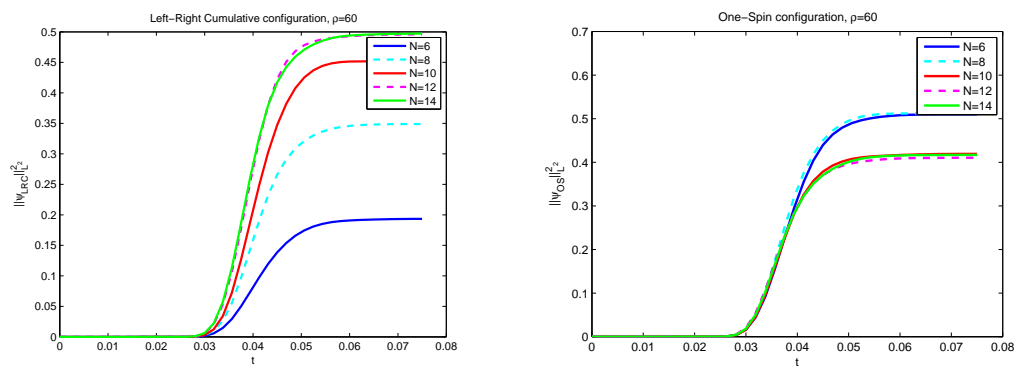

Figure 4: Plot of the $2*LRC$ and OS probabilities as a function of t, for $\rho = 60$ and several spin-detectors N.
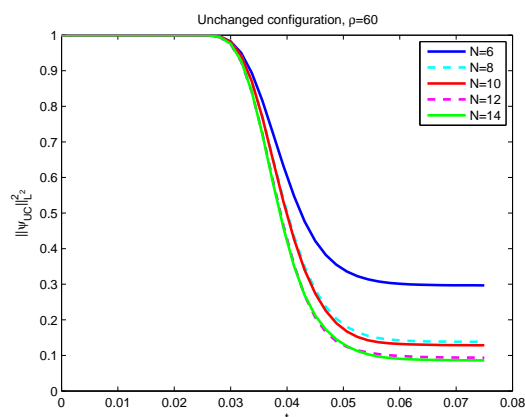
Figure 5: Plot of the UC probability as a function of t, for $\rho = 60$ and several spin-detectors N.

5 Conclusions

Aim of this paper was to give numerical results concerning the evolution of a quantum particle in a quantum environment. We modeled the environment as an array of N localized two level quantum systems interacting with the particle via a multi-channel point interaction. We considered a spatially one dimensional model where the N constituents of the environment are distributed symmetrically with respect to the origin: $N/2$ of them on the right side of the origin and $N/2$ of them localized in symmetric positions on the other side of the origin. The interaction hamiltonian was chosen in the family of the so called multi-channel point interaction hamiltonians, extensively used, since decades, in applied quantum physics [3,5,10,12,20,24].

The evolution of the whole system, made of the particle and of the spins, is completely represented as a multi-channel wave function for the particle, each channel corresponding to one of the 2^N possible quantum states of the array of spins. The initial state is chosen to belong to the channel where all the spins are in the down state (the one with minimal energy). The interaction hamiltonian allows crossing of channels when the particle has non zero probability to be in the region occupied by the spins.

The numerical analysis we performed shows that, as expected, the state of the whole system, after a short interaction time and apart from negligible terms, is the sum of three wave packets corresponding to three "macroscopically" different states:

1. no significative change in the overall spin state of the array has taken place and the particle is approximately in its initial state (no tracks);

2. a "substantial percentage" of spins on the right side of the origin changed state and the particle is going to the right (a "track" on the right of the origin);

3. a "substantial percentage" of spins on the left side of the origin changed state and the particle is going to the left (a "track" on the left of the origin).

This corresponds quite well to what is observed in a Wilson cloud chamber when a radioactive source emits an α-particle as a spherical wave state.

Our analysis suggests moreover that the probability of (1) is decreasing when the number of constituents of the environment increases, whereas the probability of a track formation is increasing. Furthermore, the probability of multiple spin flips on both sides of the origin is negligible at all times.

We plan to examine in further work some technical and fundamental open problems in the evolution of a quantum particle in a quantum environment. First of all, we would like to push the computation to the point where N is sufficiently large to allow to specify rigorously the meaning of "macroscopic change of the environment " with respect to the initial condition. We then would like to face the problem of analyzing the dependence of the results on the basis we use to represent the initial state of the particle.

Last, but not least, we plan to analyze the problem in dimension larger than one. For $d = 2$ and $d = 3$ a general definition of multi-channel point interaction is available. The numerical study in those cases is probably simplified considering the dynamical equations governing the singularities of the wave functions on the points where the spins are localized (for details see e.g [7]).

Acknowledgments

References

[1] R. Adami, M. Hauray, C. Negulescu, Decoherence for a heavy particle interacting with a light one: new analysis and numerics, submitted.
[2] Bauer M., Bernard D., *Convergence of repeated quantum non demolition measurements and wave function collapse* Phys. Rev. A **84** 044103, (2011).
[3] Cacciapuoti C., Carlone R., Figari R. Perturbations of eigenvalues embedded at threshold: Two-dimensional solvable models, *J. Math. Phys.*, **52**, 8, 083515, 2011.
[4] Cacciapuoti C., Carlone R., Figari R. A solvable model of a tracking chamber *Rep. Math. Phys.*, **59**, 3, 2007.
[5] Cacciapuoti C., Carlone R., Figari R., Spin-dependent point potentials in one and three dimensions, *J. Phys. A: Math. Theor.*, **40**, 249-261, 2007.
[6] Darwin C.G., A collision problem in the wave mechanics. *Proc. R. Soc. Lond. A*, **124**, 375-394, 1929.
[7] Dell'Antonio G., Figari R., Teta A., A brief review on point interactions. Inverse problems and imaging (Martinafranca, 2002), L. Bonilla ed. 171-189, Springer LNM n.1843,2008.
[8] Dell'Antonio G., Figari R., Teta A., Joint excitation probability for two harmonic oscillators in dimension one and the Mott problem. *J. Math. Phys.*, **49**, n. 4, 042105, 2008.

[9] Dell'Antonio G., Figari R., Teta A., A time dependent perturbative analysis for a quantum particle in a cloud chamber. *Ann. H. Poincaré*, **11**, n. 3, 539-564, 2010.

[10] Demkov Y.N., Ostrovskii V.N., *Zero-Range Potentials and Their Applications in Atomic Physics*, Plenum Pub Corp, 1988.

[11] Figari R., Teta A., Emergence of classical trajectories in quantum systems: the cloud chamber problem in the analysis of Mott (1929). *Arch. Hist. Ex. Sci.*, **67**, no. 2, 215-234, 2013.

[12] R. Figari and A. Teta, *Quantum Dynamics of a Particle in a Tracking Chamber*, Springer-Verlag (2013).

[13] Heisenberg W., Über quantentheoretische Umdeutung kinematischer und mechanischer Beziehungen. *Z. Phys.*, **33**, 879-893, 1925. Eng. trans. reprinted in: van der Waerden B.L., *Source of Quantum Mechanics*, Dover Publications, Inc., 1967.

[14] Heisenberg W., Über den anschaulichen Inhalt der quantentheoretischen Kinematik und Mechanik. *Z. Phys.*, **43**, 172-198, 1927. Eng. trans. reprinted in: Wheeler J.A., Zurek W., *Quantum Theory and Measurement*, Princeton University Press, 1983.

[15] Heisenberg W., *The Physical Principles of the Quantum Theory*, The University of Chicago Press, 1930.

[16] Hepp K., Quantum Theory of Measurement and Macroscopic Observable. *Helv. Phys. Acta*, **45**, 237-248, 1972.

[17] Hornberger K, Sipe J. E., Collisional decoherence reexamined. *Phys. Rev. A*, **68**, 2003.

[18] Joos E., Zeh H.D., The emergence of classical properties through interaction with the environment. *Z. Phys. B*, **59**, 223243, 1985.

[19] Joos E., H. D. Zeh, Kiefer C., Giulini D., Kupsch J., Stamatescu I. O., *Decoherence and the Appearance of a Classical World in Quantum Theory*, 2nd ed., Springer, 2003.

[20] Lovesey S.W., *Theory of Neutron Scattering from Condensed Matter*, vol. I, Claredon Press, 1984.

[21] Mott N.F., The wave mechanics of α-ray tracks. *Proc. R. Soc. Lond. A*, **126**, 79-84, 1929.

[22] Recchia C, Teta A., Semiclassical wave-packets emerging from interaction with an environment, J. Math. Phys., 55,1 012104, (2014).

[23] M. Schlosshauer, *Decoherence and the Quantum-To-Classical Transition* Springer-Verlag (2007).

[24] Šeba P., Exner P., Pichugin K.N., Vyhnal A., Streda P., Two-component interference effect: model of a spin-polarized transport. *Phys. Rev. Lett.*, **86**, 1598-1601, 2001.

[25] Sewell G., On the Mathematical Structure of Quantum Measurement Theory. *Rep. Math. Phys.*, **56**, n. 2, 271-290, 2005.

[26] Teta A., Classical behavior in quantum systems: the case of straight tracks in a cloud chamber. *Eur. J. Phys.*, **31**, n. 1, 215-227, 2010.